Drag resistance of ship hulls: Effects of surface roughness of newly applied fouling control coatings, coating water absorption, and welding seams

Wang, Xueting; Olsen, Stefan Møller; Andrés, Eduardo ; Olsen, Kenneth Nørager ; Kiil, Søren

Published in:
Journal of Coatings Technology and Research

Link to article, DOI:
10.1007/s11998-018-0054-7

Publication date:
2018

Document Version
Peer reviewed version

Drag resistance of ship hulls: Effects of surface roughness of newly applied fouling control coatings, coating water absorption, and welding seams

Xueting Wang[a], Stefan Møller Olsen[b], Eduardo Andrés[c], Kenneth Nørager Olsen[d], Søren Kiil[a,*]

[a]Department of Chemical and Biochemical Engineering, Technical University of Denmark (DTU) Building 229, 2800 Kgs. Lyngby, Denmark

E-mail: xewa@kt.dtu.dk

Telephone: +45 45 25 28 00

[b]Department of Fouling Release Systems, Hempel A/S, Lundtoftegårdsvej 91, 2800 Kgs. Lyngby, Denmark

E-mail: stmo@hempel.com

Telephone: +45 45 93 38 00

[c]Department of Fouling Control, PINTURAS HEMPEL S.A.U., Carretera Sentmenat 108, 08213 Polinyà (Barcelona), Spain

E-mail: edan@hempel.com

Telephone: +34 937 284 909

[d]Maersk Line, Esplanaden 50, 1098 Copenhagen K, Denmark

E-mail: kenneth.norager.olsen@maersk.com

Telephone: +45 33 63 58 14

[*]Corresponding author, e-mail: sk@kt.dtu.dk, telephone: +45 45 25 28 27

Abstract

Fouling control coatings (FCCs) and irregularities (e.g. welding seams) on ship hull surfaces have significant effects on the overall drag performance of ships. In this work, skin frictions of four newly applied FCCs were compared using a pilot-scale rotary setup. Particular attention was given to the effects of coating water absorption on skin friction. Furthermore, to investigate the effects of welding seam height and density (number of welding seams per five meters of ship side) on drag resistance, a new flexible rotor was designed and used for experimentation.

It was found, under the conditions selected, that a so-called fouling release (FR) coating caused approximately 5.6 % less skin friction (torque) over time than traditional biocide-based antifouling (AF) coatings at a tangential speed of 12 knots. Furthermore, results of immersion experiments and supporting “standard” water absorption experiments showed that water absorption of the FR coating did not result in any significant impacts on skin friction. On the other hand, water absorption was found to actually lower the skin friction of AF coatings. This may be attributed to a smoothening of the coating surface.

The effects of welding seam height and density on drag resistance were found to be substantial when welding seam height is above 5 mm, especially at high tangential speeds (above 15 knots). Using an interpolation approach, the pilot-scale welding seam drag data could be used to estimate the drag resistance at approximated full-scale conditions, equivalent to about one welding seam per five meters of ship side. It was shown, in this case, that the contribution of welding seams to ship skin friction could very well be less significant than those of FCCs when the welding seam height is below 5 mm, a representative value for full-scale welding seam height.

Keywords

Drag resistance, fouling control coatings, water absorption, welding seam height, welding seam density

Introduction

Marine biofouling is known as the undesirable accumulation of marine species, such as bacteria, algae, slime, seaweed, barnacles and tubeworms, on any surfaces immersed into seawater. It has long been a global challenge, in particular for the naval industry, because of both economic and environmental issues.[1-3] Consequences of biofouling have been elucidated in previous reports,[2,4-6] and one of the most important is the increased drag resistance which leads to a higher fuel consumption.

Drag resistance has been studied since the 1970s[7-11] and recently reviewed.[12] Previous investigations related to drag resistance have been mainly focused on evaluation of drag penalties,[13] prediction of drag resistance,[14] and drag characterization methods.[8,11,15,16] Among all, prediction of drag resistance is still a crucial topic.[14,17] The total drag resistance for a marine vessel is composed of three parts. The major part is skin friction, which accounts for 70-90 % of the total drag resistance for slow trading ships (e.g. tankers) and typically less than 40 % for faster trading ships (e.g. container ships).[12] The remaining part is primarily attributed to wave and eddy formation, the so-called residuary resistance. Air resistance, above the waterline, normally constitutes a minor portion of the total drag resistance, often 2 % or less for slow trading ships and 10 % or less for faster trading ships.[18] Schultz reported that the hull conditions, including coating roughness and biofouling, have direct effects on skin friction while the influence on residuary resistance is negligible.[19]

To prevent biofouling, a large number of potential methods have been investigated (see e.g. Swain[20], Callow[21]). However, so far, the most successful approach has been to apply FCCs to underwater ship hull surfaces. Two major fouling control coating technologies have been developed over the years. The conventional biocide based antifouling (AF) coatings release active compounds into seawater in a controlled manner; whereas the so-called fouling release (FR) coatings, which possess

low surface energy, flexible mechanical properties and have smooth surfaces, minimize the adhesion between marine organisms and coating surface so that the marine organisms can be removed by hydrodynamic forces during sailing or an occasional scrubbing. Their developing history and working mechanisms have been described in previous reviews[3,4,6] and will not be discussed in detail here. Recent findings on fouling control technologies are provided by e.g. Oikonomou et al.[22], Yonehara et al.[23].

The newly applied FCC surface roughness is of primary importance to the drag performance of marine vehicles and the effects of coating surface roughness on skin friction have been investigated in previous studies[8,24] and detailed by Schultz and co-workers.[19,25,26] Schultz et al. also reported that skin friction can account for 90 % of the total drag resistance when the coating surface is still free of fouling.[2] Therefore, it is of great interest to compare the effects of surface roughness of different newly applied FCCs on skin friction. Few relevant works have been published so far. Lindholdt et al.[14] mentioned that the skin friction difference is significant. Moreover, from ship owners, we have been informed that fuel consumption differences between two FCC technologies have been observed: ships applied with FR coatings consume less fuel than those with AF coatings and the effect can last for months until biofouling growth becomes decisive for the fuel consumption. Therefore, in this work, the skin friction among different newly applied FCCs will be compared and the influence of the difference will be evaluated economically.

Meanwhile, it is important to point out, that water absorption of FCCs is inevitable. Consequently, the drag performance of FCCs may be affected by water absorption of the coating film. However, no relevant studies have been reported so far. Therefore, to verify the hypothesis, the effects of water absorption of newly applied FCCs on skin friction will be investigated in the present work by conducting both immersion experiments and “standard” water absorption tests. From the immersion

experiments, the effects of coating surface roughness of two FCC technologies on skin friction can be compared.

Another source of drag resistance is large surface irregularities formed on ship hull surfaces during the ship construction process. Compared to the effects of coating surface roughness on skin friction, large surface irregularities may affect drag resistance more significantly in a different way. An investigation by Weinell et al. showed that the contribution of hull coatings to skin friction is negligible compared to large surface irregularities.[11] Therefore, it is important to compare the contribution of coating surface roughness to the overall drag resistance with that of large surface irregularities. One common surface irregularity is welding seams which are normally formed on the ship hull surfaces when two steel plates are welded together, typically ending up with irregular shapes, even though welding seams are constructed according to different standards. The quality of welding seams varies, mainly depending on the welding seam height (from 3 to 9 mm) and welding seam density on the ship hull surfaces. Previously, the effects of welding seam height on drag resistance have been investigated using an approach of computational simulation.[27] However, no experimental work has been reported so far. Therefore, in the present work, the effects of both welding seam height and density on drag resistance will be studied through an experimental approach. The effects of coating surface roughness on drag resistance will be compared to those of welding seams.

Experimental equipment for estimating drag resistance was summarized in the review by Lindholdt et al.[12] Setups with rotating cylinders have been used to estimate drag resistance[9,11,14,28] and will also be used in the present work. One of the main hypotheses is that the rotary setup is sensitive enough to small surface roughness changes so that the corresponding changes in skin friction of different FCCs, after water immersion, can be estimated and compared. The biofouling process will not be

part of this work and only welding seams perpendicular to the water surface was considered because the horizontal welding seams have less significant effects on drag resistance.

Experimental setup

All drag resistance investigations were performed using a pilot-scale rotary setup as shown in figure 1 (left), which contains two concentric cylinders with the inner cylinder rotating. The purpose is to create a close approximation to Couette-flow between two parallel walls of the two cylinders. In this case, one wall moves at a constant velocity and the wall shear stress is comparable to that of a real ship.[29] For further details on the setup see Weinell et al.[11] and Lindholdt et al.[12,14]

In the present investigation, fouling control coating samples were applied to the outer surface of cylindrical rotors as shown in figure 1 (middle). Subsequently, the coated rotors were mounted onto the shaft of the rotary setup and then immersed into a tank (the diameter of the tank is 0.82 m) containing 600 liters of artificial seawater, following the preparation method descried by Lyman and Fleming.[30] This method was chosen as it is one of the most widely used recipes for artificial seawater. Demineralized water was added every week to the tank to compensate for water evaporation. A KEB frequency converter (type 12.F4.S1E-3440) was used to adjust the rotation speed. Due to heat generated from rotation of the rotor, the temperature of the seawater may increase, and this was avoided using water bath cooling. Isothermal conditions were attained by a cold water bath, which removed the heat generated from rotation of the rotor. The cold water bath is connected to a spiral pipe mounted near the inside wall of the tank. A torque sensor installed on the shaft recorded the torque values generated during the rotation. These values were used to estimate the drag resistance.

Torque measurements have been used to estimate drag resistance of objects and surfaces since the 1970s.[12,15] The conversion from values of torque to skin friction coefficients can be done using equations for wall shear stress, and an assumption of torque values being directly related to the wall

shear stress.[14] Therefore, even though no actual towing tank ("drag") experiments were done in this work, we use the term "drag resistance" when we discuss the results.

Due to the fact that it was not possible to correct for the contribution to the torque from top and bottom surfaces, the outer shaft surface, and the presence of bearings for the welding seam rotor (introduced below), the total torque only was measured and later presented. This means that relative comparisons are possible. However the absolute drag (torque) values for the individual coatings and welding seams cannot be extracted.

Figure 1. The full pilot-scale rotary setup for drag resistance measurements (left), cylindrical rotor (made of polyvinyl chloride) used in the rotary setup (shown without a coating applied) (middle) and the flexible rotor (made of polyoxymethylen) with six artificial welding seams (made of polyvinyl chloride, the grey parts in the photo) on the outer surface (right).

Flexible cylinder

A flexible cylinder as shown in figure 1 (right), was designed to simulate welding seams on ship hull surfaces. The dimension of the flexible cylinder is 0.3 m in diameter and 0.31 m in height. The diameter of the outer static cylinder (not shown) mounted inside the tank is 0.38 m. Therefore, the gap between the flexible cylinder and the outer static cylinder is 40 mm. The artificial welding

seams were constructed with a width of 15 mm according to the information provided by A.P. Møller - Mærsk A/S. Four welding seam heights (0, 3, 5 and 9 mm) were used in the study. The cylinder without welding seams (height=0 mm) was used as reference. The artificial welding seams were attached to the cylinder via grooves cut into the cylinder and with two fixation bolts at each end. A maximum of eight welding seams can be used on the cylinder. The materials of the flexible cylinder and the artificial welding seams are polyoxymethylen and polyvinyl chloride (PVC), respectively.

The flexible rotor allows investigating the effects of both welding seam height and density on drag resistance. Basically, the density of the welding seams was controlled by the number of welding seams mounted on the outer cylinder surface. For reasons of balance, the number of welding seams on the rotor could be 0, 2, 4, 6 and 8, corresponding to welding seam densities of 0, 10, 20, 30 and 40 welding seams per 5 m ship side, respectively. The unit for welding seam density was chosen for convenience of comparison between lab-scale and full-scale. The aforementioned welding seam densities (except zero) are much higher than that on full-scale ships (typically one welding seam per 5 m ship side) because the welding seam density is limited by the relative short circumference of the rotor cylinder. However, as it will be further discussed in the results and discussion section, it is possible to interpolate between data points to find the relevant full-scale drag resistance values. Note, that the welding seam density in the ship bow region can be high with 2 to 3 welding seams per 5 m.

The somewhat irregular welding seams found on real ship hull surfaces were approximated by an arc shape as shown in figure 1 (right). It was assumed that the welding seams on the flexible rotor do not affect each other and that the cylindrical geometry has no effect on drag resistance (relative to flat plate geometry as on ships). The latter assumption is reasonable as discussed in Lindholdt et al.[12] However, the former is questionable when going to high welding seam densities[31] and will be

discussed further in a later paragraph. During the experiments with welding seams, no coating was applied on the flexible rotor cylinder surfaces.

Materials and experimental procedures

Seawater immersion experiments

Four commercial fouling control coating formulas were investigated, as listed in table 1, with the purpose of comparing two fouling control coating technologies (AF and FR coatings) and investigating the effects of water absorption on skin friction using the pilot-scale rotary setup. Hempaguard X7 acts as a FR coating, while the other three are AF coatings. In all coatings used, xylene was the main solvent. Acrylic binders and rosins were used in three AF coatings. Besides, three AF coatings contain bioactive pigments (mainly cuprous oxide) and coloring pigments (mainly iron oxide). Hempaguard X7 contains silicone as binder and a small amount of copper pyrithione as bioactive pigment. The sample of Hempaguard X7 was composed of two layers of coatings, one layer of tie-coat followed by one layer of silicone topcoat. The sample of Dynamic was comprised of one layer of tie-coat followed by two layers of antifouling topcoat. Globic 9000 and Olympic+ included one layer of tie-coat and one layer of antifouling topcoat. The temperature was controlled by a water cooling bath and fluctuated ±2 °C during the experiments. It was assumed that the temperature fluctuation was too small to affect the measurements.

Table 1. Immersion conditions for each of the studied commercial FCCs.

Fouling control coating samples	**Tangential speed (RPM)**	**Temperature (°C)**	**Immersion time (Days)**
Hempaguard X7 89900 (FR)	400±1	20±2	49
Hempel's Antifouling Dynamic 79580 (AF)	400±1	20±2	49
Hempel's Antifouling Globic 9000 78900 (AF)	400±1	19±2	50
Hempel's Antifouling Olympic+ 72900 (AF)	400±1	19±2	50

The four fouling control coating samples were sprayed (airless) manually on four PVC cylinders by the same person and left to dry at room temperature. The immersion started after they were fully

dried/cured (approximately one week). Once immersed, the initial skin frictions were measured immediately and their torque values at various tangential speeds were obtained. After the first measurement, each sample was measured almost once per day in the first week. Afterwards, each sample was measured every two or three days. All the rotors were immersed statically and rotated only when measurements took place. Notice, that only one cylinder for each coating was prepared and at least three repetitions were done for each coated cylinder to obtain standard deviations for the daily measurements.

"Standard" water absorption tests

Water absorption experiments were conducted for samples Hempaguard X7, Dynamic and Globic 9000. The coating samples of Dynamic and Globic 9000 were applied on polycarbonate panels without primer by a Doctor Blade applicator. The sample of Hempaguard X7 was applied with a primer. The gap of the applicator blade used was 300 μm for all samples. Afterwards, for the Dynamic and Globic 9000 coating samples, the panels were dried for 24 h at room temperature followed by 72 h at 45 °C; for the Hempaguard X7 coating sample, the panel was dried for several days at room temperature followed by 72 h at 45 °C. For each coating formula, three replicates were conducted. A blank panel was used as reference because the panel itself absorbs water. Artificial seawater (the same as used in the above mentioned immersion experiments) was used for all the experiments. The temperature used for absorption was 23 °C and for desorption it was 60 °C.

The principle of the water absorption experiments is to weigh the panels regularly to calculate the water uptake. It should be noticed that soluble ingredients in AF coatings (e.g. cuprous oxide) will dissolve and be released during the immersion. All the panels were immersed statically for 28 days in total and weighed once per day in the first three days. After one week, the coated samples were weighed only once a week. For convenience of comparison, the unit of the water absorption was taken as g/(m^2 of coating).

Welding seam experiments

To determine the effects of welding seam height and density on drag resistance and compare with the effects of FCCs, a series of welding seam experiments were performed using the new flexible cylinder with the pilot-scale setup (Table 2).

For each welding seam height experiment, 2, 4, 6 and 8 welding seams were attached to the flexible cylinder and studied individually. Non-used empty grooves were filled with welding seams of zero mm height as shown for one of the seams in figure 1 (right). For welding height of zero mm, all 8 welding seams must be attached. For verification, the original intact cylinder with a smooth surface before cutting was also measured at each speed. The differences between the intact cylinder and the cylinder with 8 welding seams of zero mm are the joint lines after welding seams are mounted into grooves.

For each experiment, various tangential speeds were applied up to 20 knots and three replicates were performed at each speed. Note that speed indications refer to tangential speeds rather than ship speeds. The Reynolds number for approximated Couette-flow at 20℃ was calculated based on the equation described by Arpaci and Larsen[32] and found to be 59810 for 100 RPM (corresponding to a tangential speed of 1.57 m/s or 3.05 knots). Therefore, the flow is turbulent.[33]

Table 2. The experimental series for the flexible rotor under conditions of approximated Couette-flow (14 experiments).

Welding height (mm)	**Welding seam numbers**			
0	0 (the intact cylinder)		8	
3	2	4	6	8
5	2	4	6	8
9	2	4	6	8

The gap between the parallel walls of the two cylinders is 40 mm which is relatively small considering the highest welding height of 9 mm. For further validation, the effects of FCCs measured under approximated Couette-flow condition were compared with experiments performed

in the absence of the outer cylinder (Table 3), in which case the distance from the tank wall to the cylinder wall was 0.26 m.

Table 3. The experimental series for the flexible rotor without the outer cylinder (5 experiments).

Welding height (mm)	Welding seams numbers	
0	8	
5	2	8
9	2	8

Results and discussion

In this section, the transient effects of water absorption of FCCs on skin friction are presented and discussed. In addition, skin friction of two commercialized fouling control technologies is compared at newly applied coating conditions. Furthermore, the effects of welding seam height and density on drag resistance are demonstrated and discussed. Finally, the effects of welding seams and FCCs on drag resistance are compared at full-scale conditions.

Seawater immersion experiments and "standard" water absorption tests

To investigate the effects of water absorption of FCCs on skin friction and compare the skin friction of two commercialized antifouling technologies, seawater immersion experiments and "standard" water absorption tests were conducted. Results of the seawater immersion experiments are shown in figures 2 and 3 and those of water absorption tests in figure 4. Each data point is the average of three replicates and the standard deviations from the three replicates are indicated by the error bars shown in figure 4. The standard deviations represented by error bars as shown in figure 2 and 3 are from three repetitions of the torque measurements.

Figure 2 shows that Hempaguard X7 gives a smaller torque than Dynamic and the average torque value of Hempaguard X7 over time (around 5.1 Nm) is approximately 5.6 % less than that of Dynamic (around 5.4 Nm) at a tangential speed of 12 knots. Therefore, it can be roughly estimated that in real life conditions, newly applied FR coatings cause less skin friction than newly applied

AF coatings at the same sailing speed, which is also in agreement with observations from Lindholdt et al.[14] and Mirabedini et al.[34]

Furthermore, it can be seen in figure 2 that the torque values of Hempaguard X7 did not vary significantly during immersion despite of some fluctuations. On the other hand, the water absorption amount of Hempaguard X7 is substantial as shown in figure 4. Therefore, it can be inferred that although water absorption of newly applied FR coatings occurs, the surface of FR coatings will not be subjected to prominent changes and the skin friction will not be significantly affected.

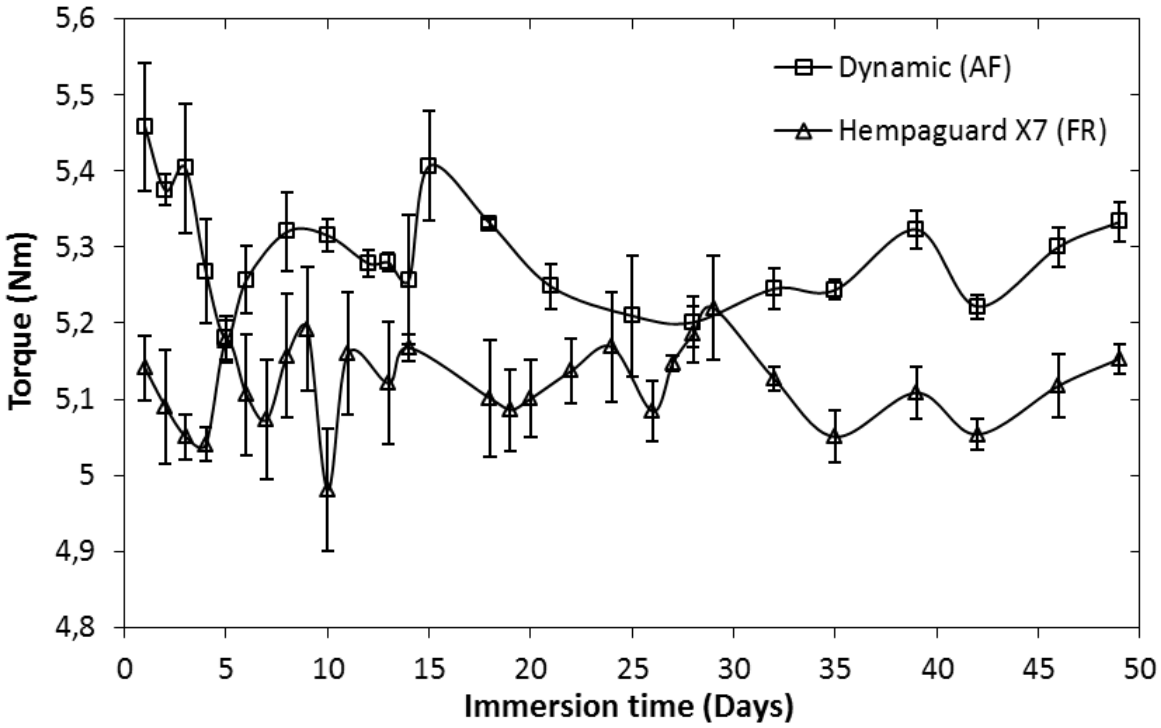

Figure 2. The average torque values of daily measurements for the newly applied Hempaguard X7 and Dynamic coatings during their entire immersion periods at a temperature of 20±2 °C and a tangential speed of 400±1 RPM (approximately 12 knots). The error bars shown represent the standard deviations of the torque measurements (at least three repetitions were used for each coated

cylinder).

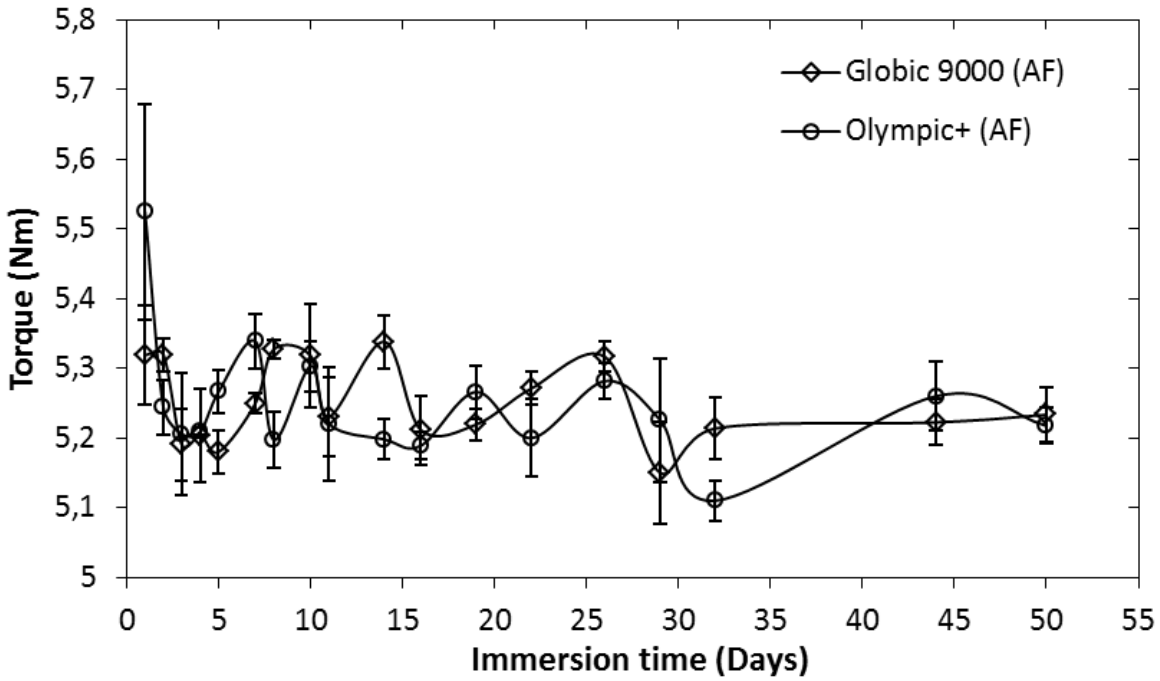

Figure 3. The average torque values of daily measurements for the newly applied Globic 9000 and Olympic+ coatings during their entire immersion periods at a temperature of 19±2 °C and a tangential speed of 400±1 RPM (approximately 12 knots). The error bars shown represent the standard deviations of the torque measurements (at least three repetitions were used for each coated cylinder).

However, a torque drop (around 0.3 Nm) is observed during the first five immersion days for the three AF coating samples as shown in figures 2 and 3. This can be seen as a self-smoothening process. Meanwhile, the amount of water absorption of the AF coatings was found to be prominent in the first week of immersion as shown in figure 4. Therefore, we believe that water absorption most likely acted as the trigger for the reduction in torque. Water absorption may cause swelling of the wetted coating surface, which may smooth the initial surface imperfections. Another possible

reason could be that water absorption triggers the polishing process, as explained below, and that the polishing can have a higher impact on the more exposed areas.

After immersion, water will penetrate into the AF coating film and soluble compounds of AF coatings will be gradually dissolved and released into water. Hence, the increasing amount of absorbed water in the first week of immersion observed in figure 4 may be attributed to the water absorption amount being accumulated faster than the release of soluble compounds. After one week, the paths inside the coating film available for water to penetrate are saturated and therefore further water absorption stops. Water absorption and the release of soluble compounds may equilibrate.

Furthermore, after the release of the soluble compounds from the AF coating film, a porous leached layer will be formed gradually at the coating-water interface.[28] During the rotation in the immersion experiments, the leached layer formed may be polished away if sufficiently vulnerable because of the velocity-dependency.[29,35] After polishing, a new front layer will be exposed to seawater. No polishing is expected in the "standard" water absorption experiments because the samples were immersed stagnantly in seawater.

As mentioned earlier, Hempaguard X7 contains small amount of biocides which have extremely low solubility in artificial seawater where the samples were immersed. Consequently, most of the biocides in Hempaguard X7 will not dissolve during the experimentation period. That is one of the reasons why it has higher water absorption compared to the two AF coatings as shown in figure 4. However, the main reason for the big difference in water absorption is a distinct difference in the binders and generic technologies between FR and AF coatings. After the first week of immersion, Hempaguard X7 reached the maximum water absorption (saturation), and no further water ingress took place.

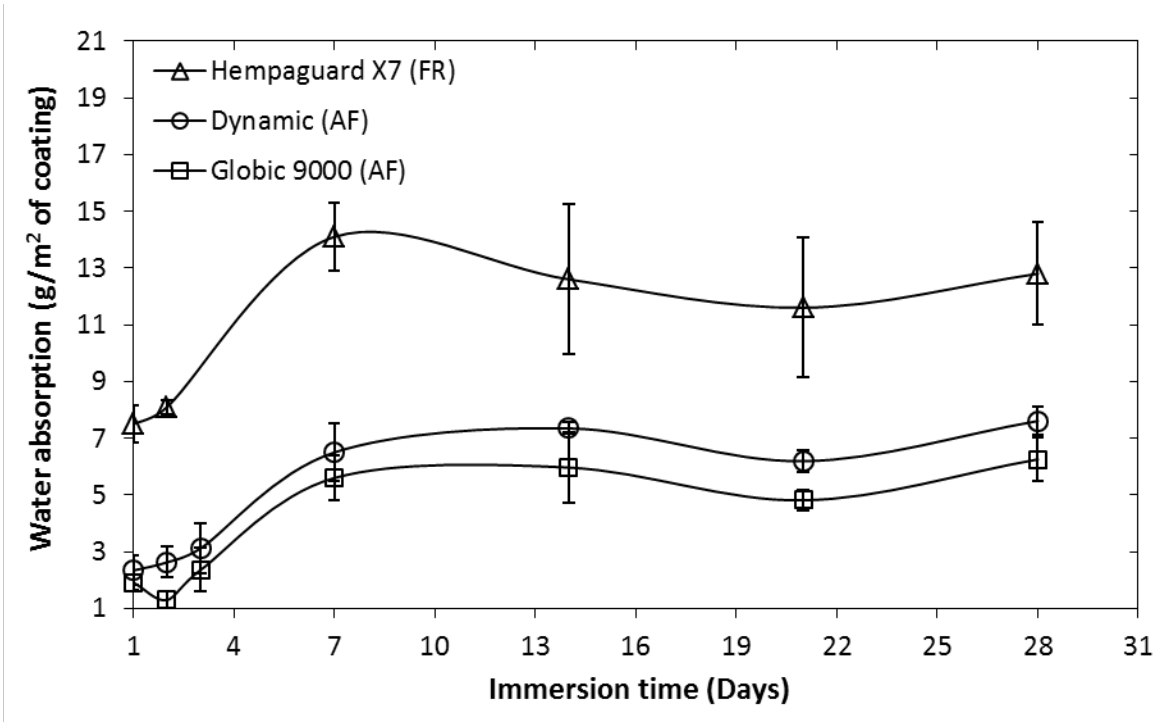

Figure 4. Water absorption of Hempaguard X7, Dynamic and Globic 9000 coatings as a function of immersion time. Each data point is the average value of three replicates. The error bar for each data point shown is obtained from the standard deviation of three replicates.

Welding seam experiments

To determine the effects of welding seam height and density on drag resistance and compare with the effects of FCCs, a series of welding seam experiments were performed using the flexible cylinder. The results are shown in figures 5-12. Each data point is the average of three replicates and the standard deviations from the three replicates are indicated by error bars shown in figures 5-8 and 10, however, note that most error bars are too small to be seen.

Two experiments were performed for a welding height of zero mm to allow comparison with a smooth reference and to evaluate any effects on drag resistance of the new joint lines after the welding seams were mounted into the grooves. The first experiment was conducted using the intact rotor cylinder before the grooves were cut and the second was performed using the rotor cylinder

after mounting eight welding seams with welding height of zero mm to the grooves. The results of the two experiments are shown in figure 5.

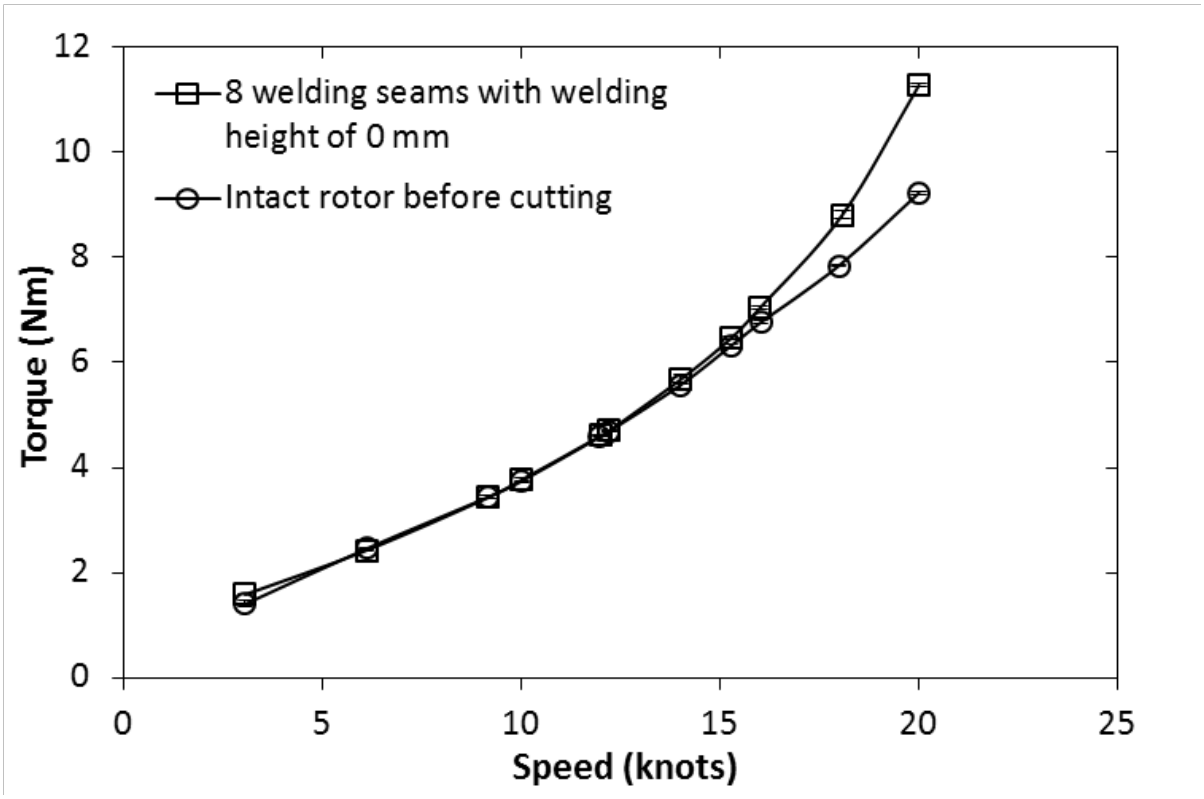

Figure 5. Comparison of torque values between the two experiments for a welding height of zero mm.

It can be seen in figure 5 that the torque values are nearly the same in the two experiments when the tangential speed is within the range of 5-15 knots, while some deviations are evident at higher speeds. Therefore, the rotary setup is sensitive to very small surface changes. Furthermore, the impact of surface obstacles on torque becomes more significant at high speeds.

The effects of welding height on torque measurements are shown in figure 6. Clearly, torque values increase when the welding height and the tangential speed are increased. Similar results were found for welding seam numbers of 2, 4, and 6 (not shown).

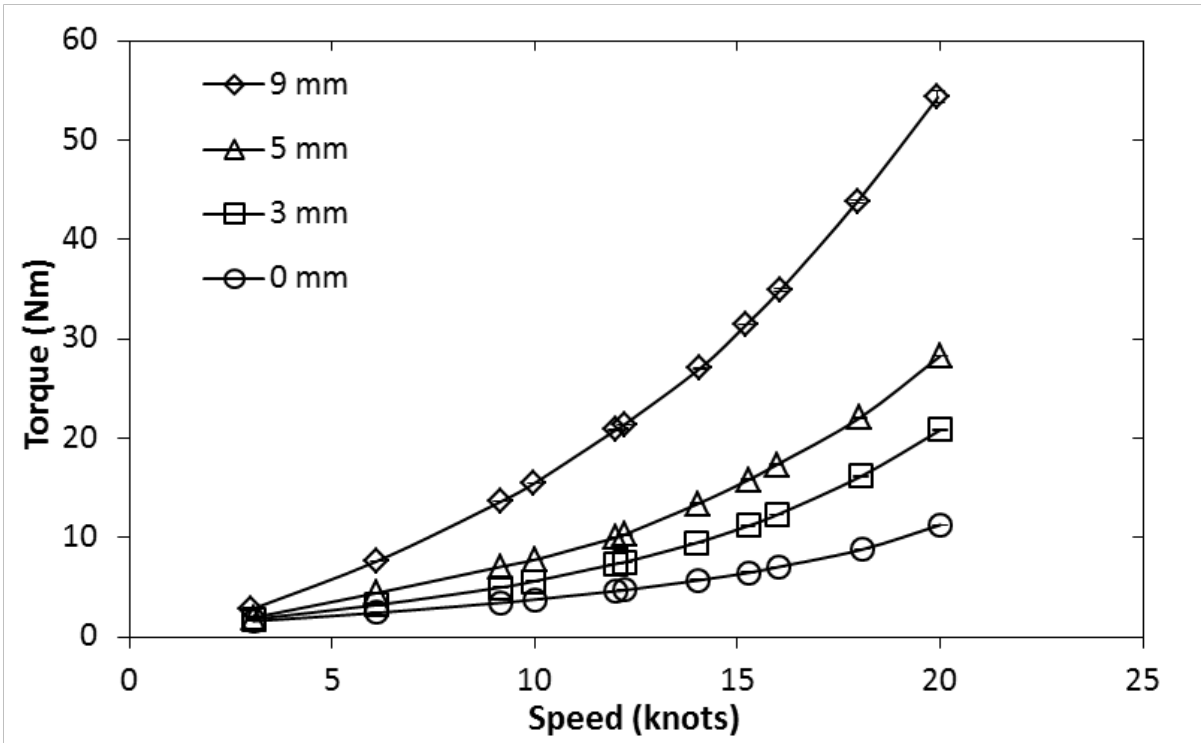

Figure 6. Torque values measured for different welding seam heights (0, 3, 5, 9 mm) with 8 welding seams mounted as a function of tangential speed.

The effects of welding seam density on drag resistance were studied as well and the results are shown in figure 7 for a welding height of 9 mm (left) and 3 mm (right). Density is seen to have a strong influence on the torque values, especially at high speeds. Furthermore, when the welding height is 9 mm, the effect of welding seam density is most significant when welding seam density is increased from 10 to 20 welding seams per 5 m, which can also be seen in figure 8. However, when the welding height is decreased to 3 mm, the incremental of torque is consistent when the welding seam density is increased linearly. This can be explained by the welding seams interacting with each other as the seam density is increased. When the welding seam height is 9 mm, there is a clear "shielding effect" (i.e. each welding seam shields the one behind it). When the welding height is decreased to 3 mm, the "shielding effect" is weakened. Therefore, the aforementioned assumption,

that the welding seams do not affect each other, is not very important when the welding seam height is ≤ 5 mm.

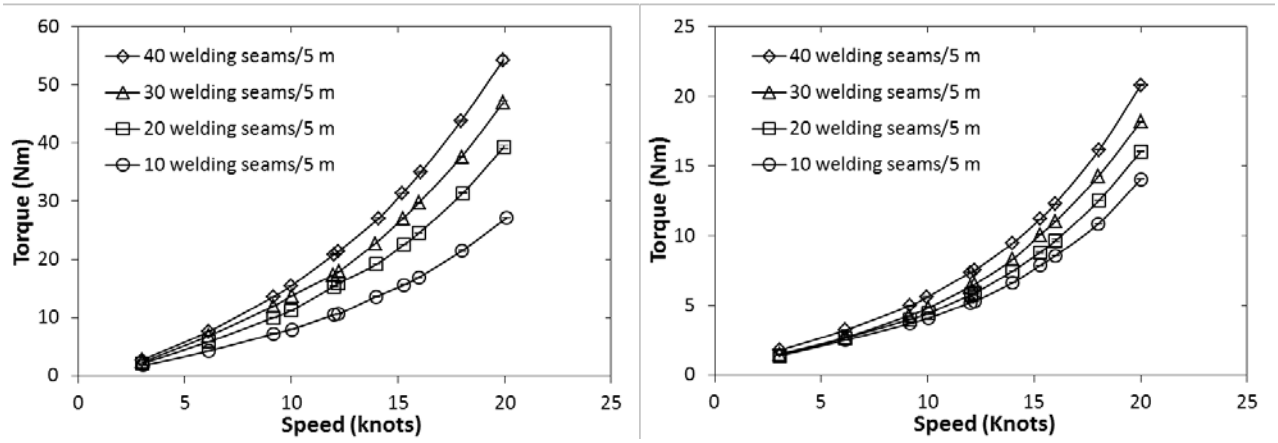

Figure 7. Torque values of different welding seam densities (10, 20, 30 and 40 welding seams/5 m) with a welding height of 9 mm (left) and 3 mm (right) as a function of tangential speed.

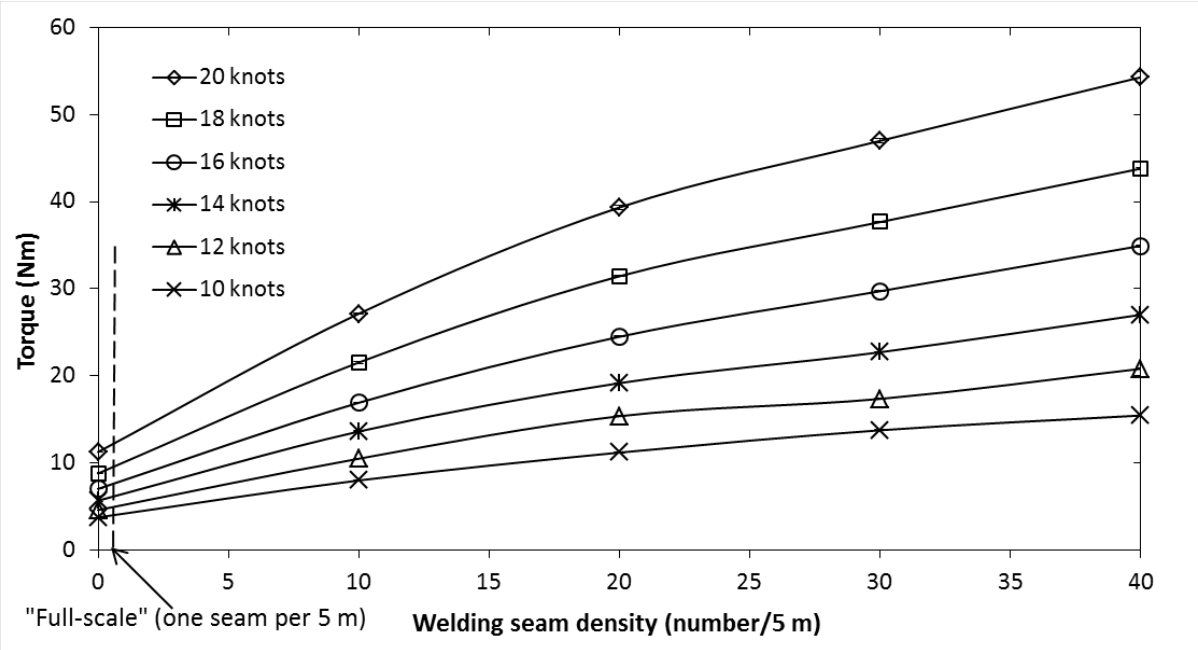

Figure 8. Torque values at different tangential speeds for a welding height of 9 mm as a function of welding seam density. The dashed line indicates a welding seam density of one welding seam per 5 m ship side, corresponding to a typical full-scale value.

To obtain torque values estimating typical full-scale conditions, the data from figure 7 have been plotted with welding seam density on the x-axis as shown in figure 8. Using an interpolation approach and assuming a linear curve between 0 and 10 welding seams per 5 m, the “full-scale” values can be very crudely estimated, as indicated in the figure, where the vertical dashed line intersects the different curves. This was also done for welding heights of 3 and 5 mm and the interpolated data are shown in Figure 9. The effects of welding seam height on torque are not significant when the height is below 5 mm, which is consistent with the results shown in figure 6. If the welding seam height is decreased from 9 to 5 mm, the torque value is decreased 8.4 % at a tangential speed of 20 knots.

It should be noted that this interpolation approach can only give a crude and qualitative estimate of the full-scale values. A quantitative approach requires the same geometry of the object (cylindrical or flat ship side) and a similarity analysis that ensures the same flow conditions over the surface. It is not possible to exactly meet those requirements with the cylindrical rotary setup.

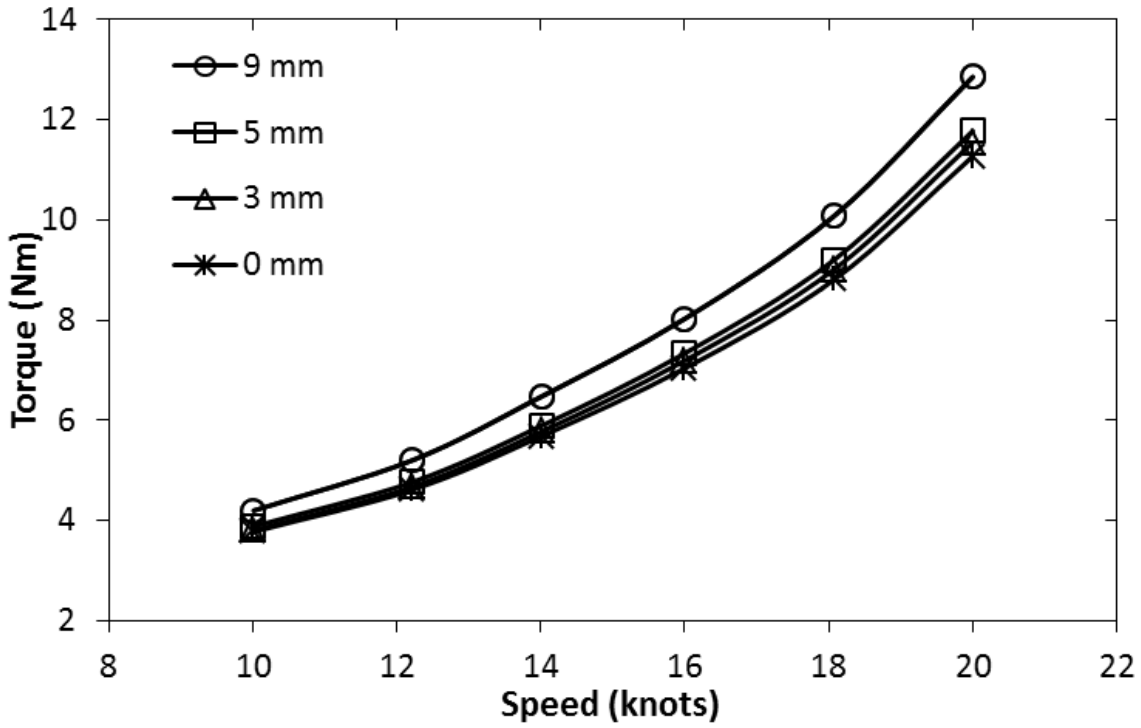

Figure 9. Interpolated torque values of different welding seam heights at full-scale welding seam density (one welding seam per 5 m ship side) as a function of tangential speed.

As discussed previously for figure 7, the assumption of individual welding seams not affecting the flow around other seams becomes questionable when the welding seam density is increased to high numbers. This could be the reason why the slopes of the lines in figure 8 start to decrease from somewhere between 10 and 15 seams/(5 m). Interaction effects should lead to less friction because the seams “shield” each other. However, this was not investigated any further because the most interesting part of the plot is the approximated full-scale conditions at very low seam density.

Experimental data for the case where the outer cylinder was absent are compared with those where the outer cylinder was present in figure 10 and 11. Figure 10 shows that the torque values of all welding seam heights are increased after removing the outer cylinder, which is most likely due to a stronger turbulence effect. The flow is now far from Couette-flow and the rotation speed could not exceed 16 knots for the 9 mm case because of prohibitive turbulence levels. Consequently, the interpolated torque values of all welding seam heights at full-scale welding seam density are increased as shown in figure 11, especially at high speeds.

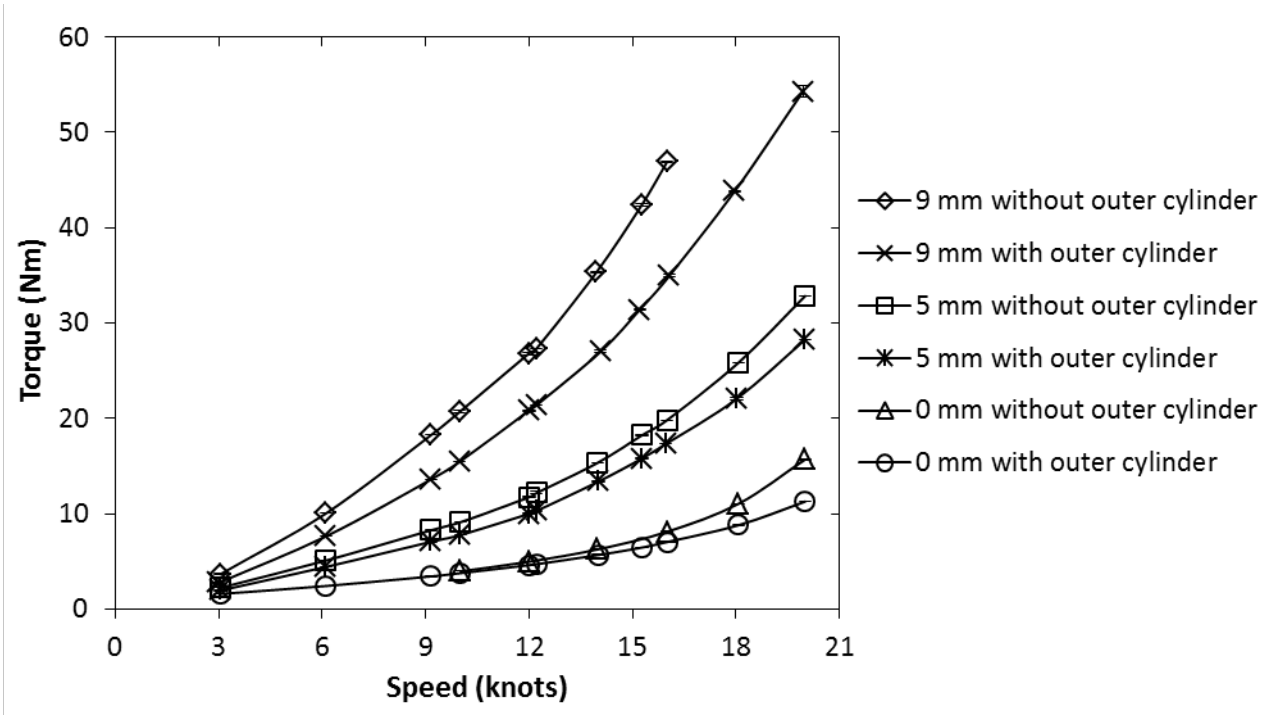

Figure 10. Comparison of torque values before and after removing the outer cylinder for welding seam heights of 0, 5 and 9 mm with 8 welding seams mounted as a function of tangential speed.

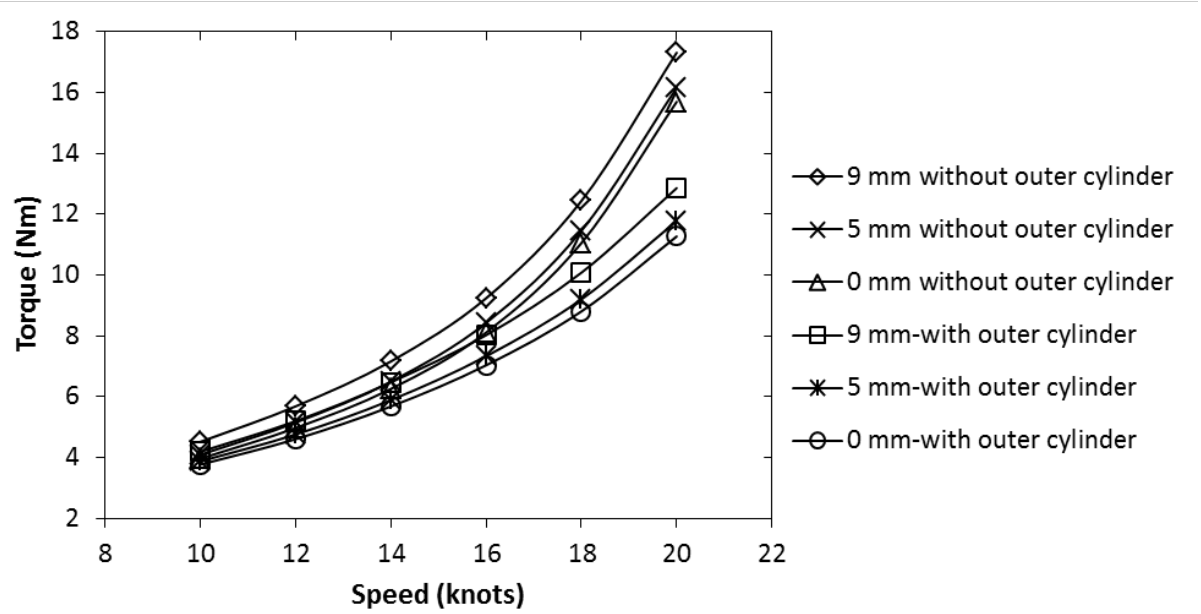

Figure 11. Comparison of interpolated torque values (to approximated full-scale conditions) before and after removing the outer cylinder for welding seam heights of 0, 5 and 9 mm at full-scale welding seam density (one welding seam per 5 m ship side) as a function of tangential speed.

Comparison of effects of coatings and welding seams on drag resistance

To compare the effects of welding seams and FCCs on drag resistance, torque values at a tangential speed of 12 knots have been summarized in figure 12. Data points for FCCs were estimated from the results of immersion experiments. It can be seen that at full-scale welding seam density, the torque values of all cylinders with FCCs are higher than those of smooth cylinders with welding seams when welding seam height is below 5 mm. Furthermore, when welding seam height is 9 mm, the torque values of all cylinders with FCCs are still equal to or higher than those of smooth cylinders with welding seams except for Hempaguard X7. Therefore, considering that the welding seam height is normally not above 5 mm, when following the European shipyard standard, both AF coatings and FR coatings will cause more drag resistance than welding seams at full-scale conditions. This is a consequence of the larger surface area taken up by coatings relative to welding seams. Notice that the torque values of FCCs were estimated from the immersion experiments at one speed only and further evidence at other speeds are needed for a more detailed analysis.

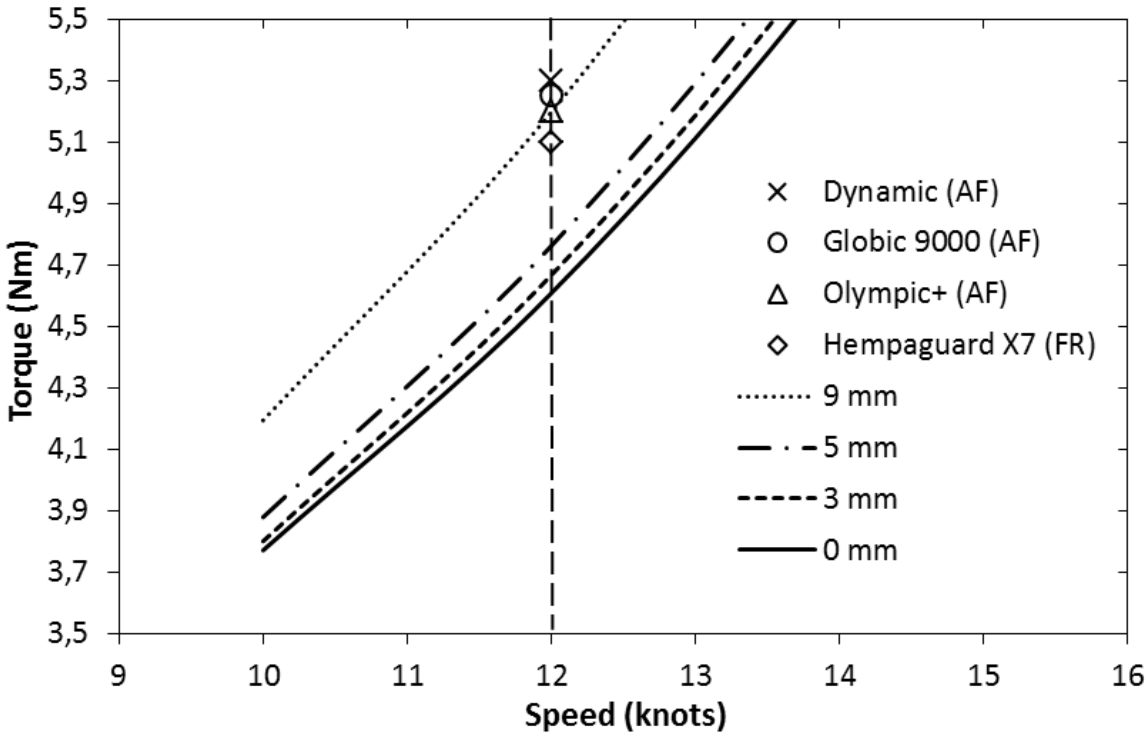

Figure 12. Comparison between torque values for different welding seam heights (Couette-flow) at full-scale welding seam density (one welding seam per 5 m ship side) and the experimental torque values of different FCCs (in the absence of welding seams) at a tangential speed of 12 knots (indicated by the dashed line).

Conclusions

In the present work, the effects of water absorption of FCCs and the presence of welding seams on drag resistance have been investigated using a pilot-scale setup with rotating cylinders. The rotary setup was found to be sufficiently sensitive to detect the impact of small changes in surface morphology on the cylinder on drag resistance and therefore the differences in drag resistance between two fouling control coating technologies were determined. It was found that the newly applied FR coating, over time, caused approximately 5.6 % less skin friction (torque) than the newly applied AF coatings at a tangential speed of 12 knots. This means that ship owners, in the initial period of ship use when the ship hull surface is still free of biofouling, can save fuel by using

FR coatings instead of AF coatings. Besides, water absorption amounts for both FR and AF coatings were found to be significant. The effects of water absorption of the newly applied FR coating on skin friction were found to be insignificant and water absorption lowered the skin friction of the newly applied AF coatings, which are crucial for FCCs because they are exposed to seawater for most of their life spans.

A flexible rotating cylinder was used to provide crude estimations of the effects of welding seam height and density on drag resistance at approximate “full-scale” conditions. It was found that the effects of welding height and density on drag resistance were significant, especially at high speeds. Besides, welding seams could interact with each other. Based on the results obtained, it was suggested that welding seam height should be controlled to less than 5 mm when ships are constructed in shipyards. This will minimize the negative effects from both welding seam height and density, especially for ships scheduled to sail at high speeds (more than 15 knots of tangential speed). Accordingly, considerable economic benefits can be achieved. Furthermore, when welding seam height is below 5 mm at full-scale conditions, FCCs were found to result in a higher drag resistance than that of welding seams at a tangential speed of 12 knots. On real ships, to reduce the impacts of welding seams, these can be ground. The economic savings related to drag reduction from grinding will be significant for welding seams of heights above 5 mm.

Acknowledgments

The authors would like to thank Antoni Sanchez, Ciaran Dunbar and Benjamin Robert Petersen for their kind help with the experiments, and Marcus Tullberg and Kim Flugt Sørensen for interesting discussions. The project is conducted under the partnership of Blue INNOship and financially supported by Innovation Fund Denmark, the Danish Maritime Fund, A.P. Møller - Mærsk A/S and Hempel A/S.

References

1. Townsin, RL, “The ship hull fouling penalty.” Biofouling, 19:S1 9–15 (2003)
2. Schultz, MP, Bendick, JA, Holm, ER, Hertel, WM, “Economic impact of biofouling on a naval surface ship.” Biofouling, 27 (1) 87–98 (2011)
3. Buskens, P, Wouters, M, Rentrop, C, Vroon, Z, “A brief review of environmentally benign antifouling and foul-release coatings for marine applications.” J. Coatings Technol. Res., 10 (1) 29–36 (2013)
4. Yebra, DM, Kiil, S, Dam-Johansen, K, “Antifouling technology - Past, present and future steps towards efficient and environmentally friendly antifouling coatings.” Prog. Org. Coatings, 50 (2) 75–104 (2004)
5. Howell, D, Behrends, B, “A review of surface roughness in antifouling coatings illustrating the importance of cutoff length.” Biofouling, 22 (6) 401–410 (2006)
6. Lejars, M, Margaillan, A, Bressy, C, “Fouling release coatings: A nontoxic alternative to biocidal antifouling coatings.” Chem. Rev., 112 (8) 4347–4390 (2012)
7. Granville, PS, “Drag-Characterization Method for Arbitrarily Rough Surfaces by Means of Rotating Disks.” J. Fluids Eng., 104 373–377 (1982)
8. Granville, PS, “Three indirect methods for the drag characterization of arbitrarily rough surfaces on flat plates.” J. Sh. Res., 31 (2) 70–77 (1987)
9. Candries, BM, Atlar, M, Mesbahi, E, Pazouki, K, “The measurement of the drag characteristics of tin-free self-polishing co-polymers and fouling release coatings using a rotor apparatus.” Biofouling, 19 27–36 (2003)
10. Candries, BM, Anderson, CD, Atlar, M, “Foul release systems and drag: observations on how the coatings work.” J. Protective Coatings & Lignin, 38-43 (2001)

11. Weinell, CE, Olsen, KN, Christoffersen, MW, Kiil S, “Experimental study of drag resistance using a laboratory scale rotary set-up.” Biofouling, 19 45–51 (2003)

12. Lindholdt, A, Dam-Johansen, K, Olsen, SM, Yebra, DM, Kiil, S, “Effects of biofouling development on drag forces of hull coatings for ocean-going ships: a review.” J. Coatings Technol. Res., 12 (3) 415–444 (2015)

13. Monty, JP, Dogan, E, Hanson, R, Scardino, AJ, Ganapathisubramani, B, Hutchins, N, “An assessment of the ship drag penalty arising from light calcareous tubeworm fouling.” Biofouling, 32 (4) 451-464 (2016)

14. Lindholdt, A, Dam-Johansen, K, Yebra, DM, Olsen, SM, Kiil, S, “Estimation of long-term drag performance of fouling control coatings using an ocean-placed raft with multiple dynamic rotors.” J. Coatings Technol. Res., 12 (6) 975–99 (2015)

15. Granville, PS, “Similarity-law characterization methods for arbitrary hydrodynamic roughnesses.” (1978)

16. Holm, E, Schultz, M, Haslbeck, E, Talbott, W, Field, A, “Evaluation of Hydrodynamic Drag on Experimental Fouling-release Surfaces, using Rotating Disks.” Biofouling, 20 (4–5) 219–226 (2004)

17. Demirel, YK, Khorasanchi, M, Turan, O, Incecik, A, “CFD approach to resistance prediction as a function of roughness.” Proc. Transport Research Arena, Paris, April 2014

18. Man Diesel & Turbo, “Basic principles of ship propulsion.” [cited on 2017, July 31]. Available from: https://marine.man.eu/docs/librariesprovider6/propeller-aftship/basic-principles-of-propulsion.pdf?sfvrsn=0

19. Schultz, MP, “Effects of coating roughness and biofouling on ship resistance and powering.” Biofouling, 23 (5–6) 331–341 (2007)

20. Swain, GW, “Biofouling Control: A Critical Component of Drag Reduction.” Proc. International Symposium on Seawater Drag Reduction, Newport, RI, USA, July 1998

21. Callow, M, “Ship fouling: problems and solutions.” Chem. Ind., (5) 123–127 (1990)

22. Oikonomou, EK, Iatridi, Z, Moschakou, M, Damigos, P, Bokias, G, Kallitsis, JK, “Development of Cu 2+- and/or phosphonium-based polymeric biocidal materials and their potential application in antifouling paints.” Prog. Org. Coatings, 75 (3) 190–199 (2012)

23. Yonehara, Y, Yamashita, H, Kawamura, C, Itoh, K, “A new antifouling paint based on a zinc acrylate copolymer,” Prog. Org. Coatings, 42 (3–4) 150–158 (2001)

24. Townsin, RL, “Estimating the technical and economic penalties of hull and propeller roughness.” Trans. - Soc. Nav. Archit. Mar. Eng., 89 295–318 (1982)

25. Schultz, MP, “The Relationship Between Frictional Resistance and Roughness for Surfaces Smoothed by Sanding.” J. Fluids Eng., 124 (2) 492-499 (2002)

26. Schultz, MP, Flack, KA, “Turbulent Boundary Layers Over Surfaces Smoothed by Sanding,” J. Fluids Eng., 125 (5) 863-870 (2003)

27. Ciortan, C, Bertram, V, “RANSE Simulations for the Effect of Welds on Ship Resistance.” Proc. Numerical Towing tank Symposium, Marstrand, Sweden, September 2014

28. Kiil, S, Dam-Johansen, K, Weinell, CE, Pedersen, MS, Codolar, SA, “Estimation of polishing and leaching behaviour of antifouling paints using mathematical modelling: a literature review.” Biofouling, 19:S1 37–43 (2010)

29. Kiil, S, Weinell, CE, Pedersen, MS, Dam-Johansen, K, “Analysis of self-polishing antifouling paints using rotary experiments and mathematical modeling.” Ind. Eng. Chem. Res., 40 3906–3920 (2001)

30. Lyman, J, Fleming, RH, “Composition of seawater.” J. Mar. Res., 3 134–146 (1940)

31. Li, L, Gao, Z, Moan, T, Ormberg, H, “Analysis of lifting operation of a monopile for an offshore wind turbine considering vessel shielding effects.” Marine structures, 39 287-314 (2014)

32. Arpaci, VS, Larsen, PS, Convection Heat Transfer. Prentice-Hall, Englewood Cliffs, NJ, USA (1984)

33. David Andereck, C, Liu, SS, Swinney, HL, “Flow regimes in a circular Couette system with independently rotating cylinders.” J. Fluid Mech., 164 155-183 (1986)

34. Mirabedini, SM, Pazoki, S, Esfandeh, M, Mohseni, M, Akbari, Z, “Comparison of drag characteristics of self-polishing co-polymers and silicone foul release coatings: A study of wettability and surface roughness.” Prog. Org. Coatings, 57 (4) 421–429 (2006)

35. Kiil, S, Dam-Johansen, K, Weinell, CE, Pedersen, MS, Codolar, SA, “Dynamic simulations of a self-polishing antifouling paint exposed to seawater.” J. Coat. Technol., 74 (929) 45–54 (2002)